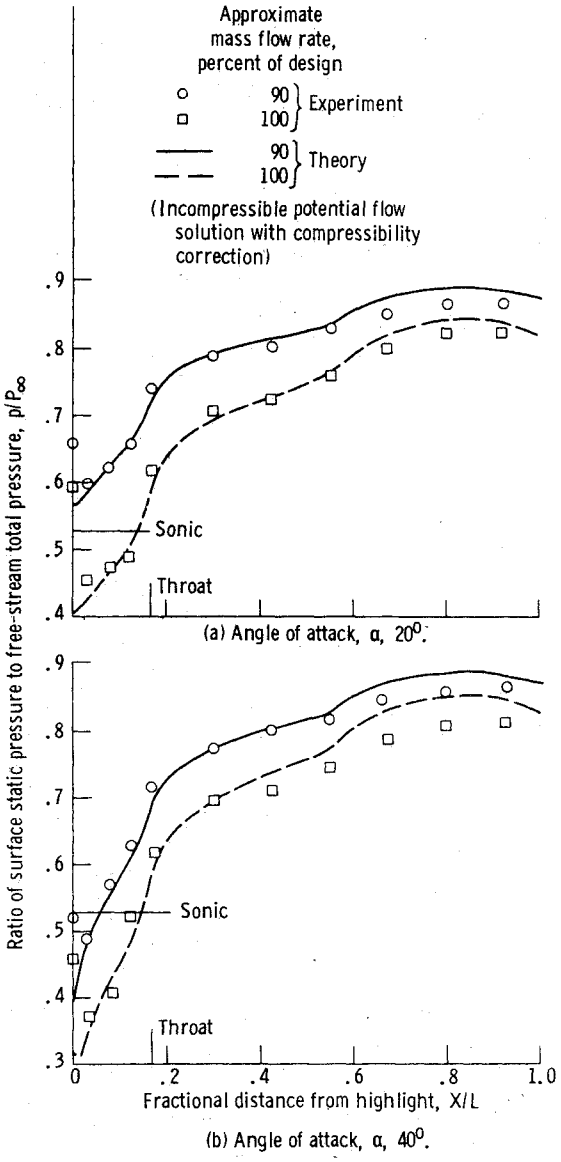

Fig. 3 Comparison of predicted internal surface static pressure distribution with experimental data for angle-of-attack conditions. Freestream velocity, $\bar{V}_\infty$, 32 m/sec.

experimental data. The possibility of local shocks and/or short separation bubbles and reattachment (often encountered on airfoils at angle of attack) near the inlet highlight could account for the experimental static pressures being higher than the theory. The discrepancy in the aft portion of the diffuser can be attributed to the neglect of the boundary-layer displacement thickness in solution which was discussed in the previous figure.

These preliminary results illustrate that the proposed compressibility correction of Ref. 1 gives a relatively good approximation to the internal compressible flow behavior and thus should be useful in the design and analysis of engine nacelle inlets. Further verification of the applicability of the compressibility correction to inlets is given in Ref. 5.

References

[1] Lieblein, S. and Stockman, N. O., "Compressibility Correction for Internal Flow Solutions," *Journal of Aircraft*, Vol. 9, No. 4, April 1972, pp. 312–313.

[2] Stockman, N. O., "Potential Flow Solutions for Inlets of VTOL Lift Fans and Engines," *Analytic Methods in Aircraft Aerodynamics*, NASA SP-228, 1970, Washington, D.C., pp. 659–681.

[3] Herring, H. J. and Mellor, G. L., "Computer Program for Calculating Laminar and Turbulent Boundary Layer Development in Compressible Flow," CR-2068, 1972, NASA.

[4] Albers, J. A., "Predicted Upwash Angles at Engine Inlets for STOL Aircraft," TM X-2593, 1972, NASA.

[5] Albers, J. A., "Theoretical and Experimental Internal Flow Characteristics of a 13.97-Centimeter-Diameter Inlet at STOL Takeoff and Approach Conditions," TN D-7185, 1973, NASA.

An Automated Procedure for Determining the Flutter Velocity

C. S. Rudisill*
Clemson University, Clemson, S.C.
and
J. L. Cooper†
Monsanto Textiles Company, Pensacola, Fla.

Introduction

EFFICIENT optimal design programs for aircraft structures which are subject to constraints on the flutter velocity require a rapid and automatic method for evaluating the flutter velocity. Lawrence and Jackson[1] described and compared three traditional methods for finding the flutter velocity of aeroelastic systems, the American approach, the British approach, and the Richardson approach. Repetitive solutions of a complex eigenvalue problem or a determinant for a large number of reduced frequencies or velocities are required for each flutter solution when traditional flutter solutions procedures such as the k-method or the p-k method[2] are employed. Bhatia[3] developed a method for solving the flutter equation and finding the match point by use of a Leguerre iteration technique. Desmarals and Bennet[4] recently developed an automated procedure for implementing the traditional V-g method of flutter solution, their method utilizes a cubic spline for interpolating generalized aerodynamic forces. In this paper a computationally efficient method for finding the flutter velocity is presented. The method utilizes derivatives of the eigenvalues with respect to the reduced frequency in a curve fitting scheme for finding the critical roots of the flutter equation. The method is unaffected by the coalescence of any of the eigenvalues.

Description of the Solution Method

The flutter equation may be written in the form

$$[K - \lambda_j(M + A)]U_j = 0 \tag{1}$$

where K, M and A are the stiffness, mass and aerodynamic force matrices respectively. λ_j is an eigenvalue and U_j is the corresponding eigenvector.

The aerodynamic force matrix is a function of the air density, Mach number, semichord, and the reduced frequency. The reduced frequency k may be defined by the relation

$$k = b\,\omega/V \tag{2}$$

Received April 13, 1973; revision received May 11, 1973. The authors wish to express their appreciation to R. V. Doggett, Jr. of the NASA Langley Research Center for his valuable suggestions in the preparation of this paper. This research was supported by NASA Research Grant NGE-41-001-027.

Index categories: Structural Dynamics Analysis; Optimal Structural Design.

*Associate Professor of Mechanical Engineering. Member AIAA.

†Development Engineer.

where b, w, and V are the reference semichord, circular frequency of oscillation and the air speed respectively.

The reciprocal of the eigenvalues may be written in the form

$$\bar{\lambda}_j = 1/\lambda_j = \chi_j + \psi_j i \,. \tag{3}$$

where $\chi_j = 1/\omega_j^2$ and $i = (-1)^{1/2}$.

A mode of oscillation has negative damping if ψ_j is positive, and has positive damping if ψ_j is negative. When any mode is undergoing steady state oscillations and is in a state of neutral stability, then $\bar{\lambda}_j$ for that mode is pure real (then $\bar{\lambda}_j$ will be referred to as a critical eigenvalue).

The critical air speeds which correspond to a critical value of $\bar{\lambda}_j$ may be found by plotting ψ_j vs ν ($\nu = V/\omega_j$) for all eigenmodes and noting the values of ν which correspond to the zero values of the ψ_j's. The smallest positive critical air speed will be referred to as the flutter velocity. Point D in Fig. 1 corresponds to a critical value of $\bar{\lambda}_3$. From a structural synthesis point of view, it is computationally inefficient to make plots of ψ_j vs ν for each flutter velocity analysis.

Instead of using the plotting procedure, the crossings of ψ_j may be approximated by fitting cubic or quadratic equations to ψ_j from computed values of ψ_j, $d\psi_j/d\nu$, and $d^2\psi_j/d\nu^2$ (equations for $d\psi_j/d\nu$ and $d^2\psi_j/d\nu^2$ are derived in the appendix). The curve fitting procedure will be described next.

Initially values of ψ_j for all eigenmodes are estimated or computed for some value of ν very near the origin (point A in Fig. 1), this point will be denoted by $(\bar{\nu},\bar{\psi}_j)$. This is done only one time at the beginning of the procedure. These values of $\bar{\psi}_j$ are used to establish a negative slope for curves of ψ_j fitted through the origin; the values of $\bar{\psi}_j$, need not be accurate since accuracy of the fitted curves is not necessary near the origin. A value of $\bar{\nu}$ equal to $1/10$ of the initially assumed critical value of ν proved satisfactory for the examples which will be discussed later. For best results (fastest convergence to a solution) the value of $\bar{\nu}$ should be selected small enough so that all $\bar{\psi}_j$'s approach zero. In a structural optimization program values of $\bar{\psi}_j$ may be computed or estimated for the initial design parameters and then used for all subsequent flutter velocity analyses.

Next, values of ψ_j and their first derivatives are computed for an initially assumed critical value of ν (point B in Fig. 1). ν, ψ_j and the first derivative of ψ_j will be denoted as ν_0, $\psi_j{}^0$ and $d\psi_j{}^0/d\nu$ at point B. The coefficients A_j, B_j and C_j of the cubic equation

$$\psi_j = A_j\nu + B_j\nu^2 + C_j\nu^3 \tag{4}$$

whose curve passes through the origin are evaluated such that the curve of ψ_j passes through point A and B with the computed slope $d\psi_j{}^0/d\nu$ at point B.

In Fig. 1 typical curves of the ψ_j for the first three eigenmodes of a system are drawn. The eigenvalues are numbered in descending order of magnitudes of the χ_j's. At points C and C′ in Fig. 1 the curves of ψ_2 and ψ_3 are discontinuous because the curves of χ_2 and χ_3 coalesce at point C″ and there is a reordering of the subscripts to the right of point C; thus, the subscripts of ψ_2 and ψ_3 are interchanged for values of ν to the right of point C. It should be noted that even though interchanging of the subscripts occurs at point C, the cubic curve will approximate the crossing for ψ_3 provided point A is close to the origin. If ν_0 had been selected to the left of point C, then a crossing of ψ_2 would have been predicted; this is not a hindrance to the method since computations are carried out in an iterative fashion in which all of the flutter modes are checked for crossover points during an iterative cycle and the lowest flutter velocity is determined for that cycle. ν_0 is set equal to the ν corresponding to the lowest flutter velocity found in the iterative cycle and then the new ν_0 is used to

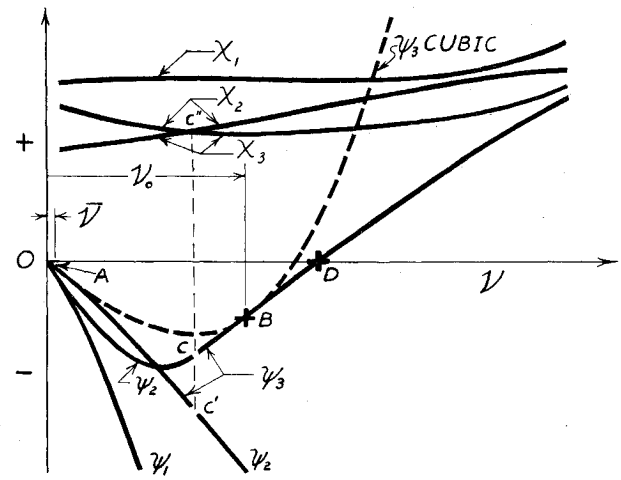

Fig. 1 χ_j **and** ψ_j **for three eigenmodes and the cubic approximation of** ψ_3.

predict crossover points for all of the modes in the next iterative cycle. This iterative procedure will cause ν_0 to converge to a value which corresponds to the final lowest flutter velocity. Obviously some of the modes do not have crossover points, for these modes the cubic equation tends to predict a crossover point where ν is either negative, zero or complex, or the flutter velocity corresponding to ν is very large. For modes which do not have crossover points, curve fitting by a quadratic equation (which will be discussed later) will tend to predict crossover points where either ν is very large, negative, or the predicted slope of ψ_j at the predicted crossover point is negative. Predicted crossover points where ν is either negative, zero or complex, or where the predicted slope of ψ_j is negative are rejected.

In each of the iterative cycles the values of all of the ω_j's are estimated from the first three terms of the Taylor's expansion of χ_j, i.e.

$$\chi_j = \chi_j{}^0 + \partial\chi_j{}^0/d\nu(\nu - \nu_0) + 0.5\partial^2\chi_j{}^0/d\nu^2(\nu - \nu_0)^2 \tag{5}$$

where $\chi_j = 1/\omega_j^2$ and the velocity at the crossing is estimated from the relation

$$V = \nu\,\omega_j \tag{6}$$

where ν is the predicted crossover value for the jth mode. The coefficients of Eq. (4) may be written in the form

$$A_j = [\bar{\psi}_j\nu_0{}^4 + \psi_j{}^0(2\bar{\nu}^3\nu_0 - 3\bar{\nu}^2\nu_0{}^2) + d\psi_j{}^0/d\nu(\bar{\nu}^2\nu_0{}^3 - \bar{\nu}^3\nu_0{}^2)]/D \tag{7}$$

$$B_j = [-2\bar{\psi}_j\nu_0{}^3 + \psi_j{}^0(3\bar{\nu}\nu_0{}^2 - \bar{\nu}^3) + d\psi_j{}^0/d\nu(\bar{\nu}^3\nu_0 - \bar{\nu}\nu_0{}^3)]/D \tag{8}$$

$$C_j = [\psi_j\nu_0{}^2 + \psi_j{}^0(\bar{\nu}^2 - 2\bar{\nu}\nu_0) + d\psi_j{}^0/d\nu(\bar{\nu}\nu_0{}^2 - \bar{\nu}^2\nu_0)]/D \tag{9}$$

where

$$D = \nu\nu_0{}^4 - 2\bar{\nu}^2\nu^3 + \bar{\nu}^3\nu_0{}^2 \tag{10}$$

The crossing of ψ_j may be found by setting ψ_j in Eq. (4) equal to zero and solving for ν, then

$$\nu = [-B_j \pm (B_j^2 - 4A_jC_j)^{1/2}]/2C_j \tag{11}$$

provided C_j is not zero and $(B_j^2 - 4A_jC_j)$ is greater than or equal to zero.

When $\psi_j{}^0$ is positive then there will be a real positive root ν of the cubic equation for which the curve will have a positive slope $d\psi_j/d\nu$ since the cubic curve for ψ_j is forced to be negative at $\nu = \bar{\nu}$.

When ν_0 is far removed from a crossover point the cubic equation may fail to predict a crossover with a real posi-

tive value of ν, in that event the quadratic equation

$$\psi_j = A_j + B_j\nu + C_j\nu^2 \tag{12}$$

is used to estimate a crossover value of ν. The coefficients A_j, B_j and C_j of Eq. (12) are computed for a curve which passes through point B of Fig. 1 and has the same first and second derivatives ($d\psi^0/d\nu$ and $d^2\psi^0/d\nu^2$) at that point. The quadratic curve does not necessarily go through the origin or the point A. The coefficients of Eq. (12) may be expressed in the forms

$$2C_j = d^2\psi_j{}^0/d\nu^2 \tag{13}$$

$$B_j = (d\psi_j{}^0/d\nu - 2C_j\nu_0) \tag{14}$$

and

$$A_j = \psi_j{}^0 - B_j\nu_0 - C_j\nu_0{}^2 \tag{15}$$

The zero roots of Eq. (12) may be found by substituting C_j, B_j, and A_j from Eqs. (13-15) into Eq. (11). If the roots for a given mode are not real and positive, then the curve fit for that mode fails.

Examples

Data for Eq. (1) was generated for the cantilevered box beam of Ref. 3 where the design parameters were those listed in Table I of that reference. The number of generalized coordinates was six. Computations were carried out on an IBM 360 model 50 machine.

A digital computer program was written which implemented the flutter velocity solution method described in Sec. 2. For the previously mentioned box beam an initial value of $\nu_0 = 1$ was assumed and the program found a flutter velocity of 869.8 fps at $\nu = 10.15$, for a tolerance ϵ equal to 0.05. The computations of the flutter velocity were repeated for values of $\nu_0 = 2, 3, \ldots, 20$. In each case the program converged to a flutter velocity between 868.2 and 870.5 for values of ν between 10.12 and 10.16. The time for the 20 flutter velocity calculations was 210.83 sec, or an average of 10.54 sec/flutter velocity analysis. For initial values of ν_0 equal to 8 and 9 the algorithm converged to an answer on the first attempt; the required time was 3.91 sec for each flutter velocity analysis. The critical mode was 2.

The flutter velocity analyses were repeated for design parameters of the box beam equal to 1/6 of the values cited in Table I of Ref. 3. The results of the flutter velocity analyses were similar to those described in the preceding paragraph.

The method was employed in the optimum design of the same box beam with six degrees of freedom and twelve design parameters of Ref. 3. ϵ was 0.05 and the total computer run time for arriving at approximately the same relative optimum design parameters of the second example of Ref. 5 was 8 min 0.00 sec. The program did not experience any convergence problems. The previous run time reported in Ref. 5 was 9 minutes 42.68 sec.

Discussion

For the first examples presented here the flutter velocity analysis program always converged to an answer for initial values of ν_0 chosen between 1 and 20 and did not show any tendency to diverge from the solution, although the curves for χ_2 and χ_3 crossed at ν equal to 8.71 where the subscripts of ψ_2 and ψ_3 switched. In the second example subscript switching did not occur for the critical mode; however, in the optimization program subscript switching occurred during several of the redesign cycles, without any noticeable effect on the efficiency or accuracy of the program.

The method for finding the flutter velocity which was presented here should be applicable to any aeroelastic flutter theory. The procedure is simple in concept and was trouble free for the examples cited.

Appendix

Equations for the first and second partial derivatives of the eigenvalues with respect to the design parameters were derived by Rudisill and Bhatia.[5] The first and second total derivatives of the eigenvalues with respect to the reduced frequency may be found by substituting derivatives with respect to the reduced frequency for derivatives with respect to the design parameters in Eqs. (15-19) of Ref. 5, then

$$\frac{d\lambda_j}{dk} = -\lambda_j V_j{}^T \frac{dA}{dk} U_j \tag{1A}$$

where $V_j{}^T[K - \lambda_j(M + A)] = 0$ and

$$\frac{d^2\lambda_j}{dk^2} = -V_j{}^T\left[\frac{2d\lambda_j}{dk}\frac{dA}{dk} + \lambda_j\frac{d^2A}{dk^2}\right]U_j + 2V_j{}^T\left[\lambda_j\frac{dA}{dk}\right]\sum_{\substack{h=1\\h\neq j}}^{n}(V_h{}^T\lambda_j\frac{dA}{dk}U_j)U_h/(\lambda_j - \lambda_h) \tag{2A}$$

where the lengths of U_j and V_j are such that $U_j{}^TU_j = 1$ and $V_j{}^T(M + A)\,U_j = 1$.

Derivatives of $\bar{\lambda}_j$ may be found from the relations

$$\frac{d\bar{\lambda}_j}{dk} = -\frac{1}{\lambda_j{}^2}\frac{d\lambda_j}{dk} \tag{3A}$$

and

$$\frac{d^2\bar{\lambda}_j}{dk^2} = \frac{2}{\lambda_j{}^3}\left(\frac{d\lambda_j}{dk}\right)^2 - \frac{1}{\lambda_j{}^2}\frac{d^2\lambda_j}{dk^2} \tag{4A}$$

References

[1]Lawrence, A. J. and Jackson, P., "Comparison of Different Methods of Assessing the Free Oscillatory Characteristics of Aeroelastic Systems," Current Paper 1084, Dec. 1968, Aeronautical Research Council, England.

[2]Hassig, H. J., "An Approximate True Damping Solution of the Flutter Equation by Determinant Iteration," *Journal of Aircraft*, Vol. 8, No. 11, Nov. 1971, pp. 885–889.

[3]Bhatia, K. G., "An Automated Method for Determining the Flutter Velocity and the Match Point," AIAA Paper 73-195, Washington, D.C., 1973.

[4]Desmarals, R. N. and Bennet, R. M., "An Automated Procedure for Computing Flutter Eigenvalues," AIAA Paper 73-393, Williamsburg, Va., 1973.

[5]Rudisill, C. S. and Bhatia, K. G., "Second Derivatives of the Flutter Velocity and the Optimization of Aircraft Structures," *AIAA Journal*, Vol. 10, No. 12, Dec. 1972, pp. 1569–1572.

Pumping Capacity of Venturi Exhausts

Jacques A. F. Hill* and Philip O. Jarvinen†
Sanders Associates Inc., Nashua, N. H.

Introduction

THE performance of a ram air operated airborne combustion unit or aircraft heater is determined largely by the amount of air which may be forced through the combustor-duct system by the differential air pressure. Venturi exhausts may be used to provide additional pressure drop across the system but may be required to pump gases with densities that differ from the pumping gas. This Note discusses experimental data on the variation of venturi

Received January 30, 1973; revision received April 18, 1973.
Index categories: Nozzle and Channel Flow; Subsonic and Transonic Flow.

* Head, AeroScience Department; now at Naval Ordnance Laboratory, White Oak, Silver Spring, Md. Member AIAA.
† Head, AeroSciences Department. Member AIAA.